Mesenchymal Stem Cell-like properties of orbital fibroblasts in Graves' orbitopathy

Katarzyna Kozdon[1], Caroline Fitchett[1], Geoffrey E. Rose[2], Daniel George Ezra[1,2¶], Maryse Bailly[1¶]

[1]Department of Cell Biology, UCL Institute of Ophthalmology, 11-43 Bath Street, London, EC1V 9EL, UK

[2]Moorfields Eye Hospital, and the National Institute for Health Research (NIHR) Biomedical Research Centre at Moorfields Eye Hospital NHS Foundation Trust and UCL Institute of Ophthalmology, UCL Partners AHSC, 11-43 Bath Street, London, EC1V 9EL, UK

Abbreviated Title: Mesenchymal stem cells in Grave's orbitopathy

Key terms: Mesenchymal stem cells, Grave's orbitopathy, orbital fibroblasts

Word count: 3875

***Number of figures and tables*: 5**

Corresponding authors and persons to whom reprint requests should be addressed:

Maryse Bailly, Ph.D

Department of Cell Biology, UCL Institute of Ophthalmology

11-43 Bath Street London, EC1V 9EL United Kingdom

Tel: 44 (0) 20 7608 6825

Email: m.bailly@ucl.ac.uk

Daniel G. Ezra, MD, FRCOphth

Moorfields Eye Hospital & the National Institute for Health Research (NIHR) Biomedical Research Centre
UCL Institute of Ophthalmology
11-43 Bath Street,
London, EC1V 9EL, UK.
Email: d.ezra@ucl.ac.uk

Support: This work was supported by Fight For Sight (grant 1341/1342 to DGE and MB). Laboratories and imaging facilities were supported by the Wellcome Trust and Fight For Sight. DE and GER acknowledge financial support from the Department of Health through the award made by the National Institute for Health Research to Moorfields Eye Hospital NHS Foundation Trust and UCL Institute of Ophthalmology for a Biomedical Research Centre for Ophthalmology. The views expressed in this publication are those of the authors and not necessarily those of the Department of Health.

Disclosure statement: The authors have nothing to disclose

Abstract

Purpose: Graves' orbitopathy (GO) is a sight-threatening autoimmune disorder causing extraocular muscle fibrosis, upper lid retraction and eye bulging due to orbital fat expansion. These clinical features are mediated by aspects of orbital fibroblasts differentiation, including adipogenesis and fibrosis. Our previous work suggested that this dual phenotype might be a manifestation of mixed cell populations, partially linked to the expression of mesenchymal stem cell (MSC) marker CD90. We thus set out to determine whether GO orbital fibroblasts displayed MSC properties.

Methods: Control and GO orbital fibroblasts previously characterised for CD90 and CD45 expression were analysed by flow cytometry for classical MSC positive (CD73, CD105) and negative (CD14, CD19, HLA-DR and CD34) markers. GO fibroblasts were further tested for their ability to undergo lineage specific differentiation following standard protocols.

Results: Both control and GO fibroblasts strongly expressed CD73 and CD105, with a higher percentage of positive cells and stronger expression levels in GO. Neither cell type express CD14, CD19 and HLA-DR. CD34 was expressed at low levels by 45-70% of the cells, with its expression significantly lower in GO cells. GO fibroblasts displayed features of osteogenesis (calcium deposits; BGLAP and SPARC expression), chondrogenesis (glycosaminoglycan production; SOX9 and ACAN expression), myogenesis (α-Smooth Muscle Actin expression) and neurogenesis (β-III tubulin expression) upon differentiation.

Conclusions: Our findings suggest that orbital fibroblasts contain a population of cells that fulfil the criteria defining MSC. This subpopulation may be increased in GO, possibly underlying the complex differentiation phenotype of the disease.

Introduction

Graves' orbitopathy (GO) is a disfiguring and potentially blinding disorder [1-3]. Clinical features include expansion and fibrosis of the orbital tissues, leading to proptosis, eyelid retraction, dry eye syndrome and diplopia [4]. At the cellular level, pathological changes include adipogenesis, fibrosis and hyaluronan production [5]. We have developed an *in vitro* model for GO using primary fibroblast cultures derived from orbital fat, which uniquely allows the study of both the fibrotic and the spontaneous adipogenic phenotype of orbital fibroblasts within 3 dimensional environments [6]. We have shown that GO fibroblasts retain a complex phenotype *in vitro*, exhibiting hyaluronan production[7], adipogenesis, and increased contractile properties and sensitivity to cytokine stimulation [6]. Orbital fibroblasts are known to comprise a mixed population of cell subtypes, including fibrocytes [8], and Thy1+/Thy1- populations, which have been proposed to underlie the adipogenic and contractile phenotype [6, 9]. Thy1 (CD90) is a major marker of stromal and adipose derived stem cells [10-12]. The high level of Thy1 expression in orbital cells in GO, as well as the diversity of the cell phenotypes observed, suggested that GO fibroblasts may possess mesenchymal stem cell-like (MSC) characteristics. We describe here how we use cell marker expression and *in vitro* differentiation to further investigate the presence of a potential MSC-like population in orbital fibroblasts.

Methods

Ethics Statement

This study was conducted according to the principles of the Declaration of Helsinki and reviewed by the National Research Ethics Service Committee London-Bentham (REC reference number 11/LO/1170). All participants gave their informed written consent before enrolment.

Cells

The 3 GO (HO1, HO2, HO3) and 3 control (CO2, CO3, CO4) orbital fibroblast lines used in this study and the clinical details of the donors have been described previously [6]. Briefly, the GO lines were derived from patients with severely active disease, having undergone prior immunosuppressive steroid treatment, whilst the control samples were from patients undergoing removal of sub-conjunctival fat herniation [6]. Unless otherwise stated, cells were grown in Dulbecco's modified Eagle's medium (DMEM, 4.5g/L L-glutamine, Life Technologies, Thermo Fischer Scientific, Paisley, UK) with the addition of 10% foetal bovine serum (FBS, Sigma-Aldrich, Gillingham, UK), 100 IU/ml penicillin, 100µg/ml streptomycin (Life Technologies, Thermo Fischer Scientific, Paisley, UK), and used between passage 3 and 8.

Flow cytometry

Subconfluent orbital GO and control fibroblasts were trypsinised and 0.3-1x10^6 cells were placed in each vial and pelleted. Cells were then resuspended in 100µl of PBS with addition of unlabelled primary (CD221, Biolegend, London, UK) or PE-conjugated (CD14, CD19, CD34,

CD73, CD105, HLA-DR, and isotype controls IgG1 and IgG2, all from BioLegend, London, UK) antibodies and incubated on ice for 1 hour. For CD221, this was followed by a PBS wash and 1 hour incubation with Cy5-conjugated goat anti-rabbit antibody (Jackson Labs, Maine, USA). Cells were washed twice with PBS, resuspended in 300µl of PBS and transferred to FACS tubes (BD Falcon, BD Biosciences, Erembodegem, Belgium). Analysis was performed using FACSCalibur (Beckton Dickinson, Oxford, UK). At least 10,000 cells were analysed per experiment, all experiments were repeated independently 3 times. The markers have been used previously to characterise multi-potent stem cells from orbital fat tissue using FACS analysis [13], [14] and are known to be insensitive to trypsin treatment [15-19], with the exception of CD14 for which immunofluorescence was used to confirm the absence of staining in orbital fibroblasts not treated with trypsin (Supplementary Figure 1, Supplementary Methods and Legends). CD73 was used as a positive control for immunofluorescence on orbital fibroblasts monolayers (Supplementary Figure 2).

Chondrogenic and osteogenic differentiation

Chondrogenic differentiation was performed as previously described [20]. Briefly, 1.25×10^6 GO fibroblasts were centrifuged and resuspended in 1ml of Chondrocyte Differentiation Medium (ZenBio, NC, USA). 200µl of the cell suspension was dispensed per well into Nunc 96-well round bottom plates. Plates were centrifuged at 500g for 5 minutes to generate a pellet and differentiation was left to proceed for 21 days with the medium changed every other day. Alcian blue staining was used to identify chondrogenic differentiation [20]. The cell pellets were fixed in formalin and embedded in paraffin. Sections were deparaffinised, and half of them were

pretreated with 0.5 mg/ml hyaluronidase (Sigma-Aldrich, Gillingham, UK) in a phosphate buffer pH 6.7. All sections were then stained with 1% alcian blue 8GX (TCS Biosciences, Botolph Claydon, UK) in 3% acetic acid glacial (Fischer Scientific, Thermo Fischer Scientific, Paisley, UK). For osteogenic differentiation, GO fibroblasts were plated in 6 well plates ($3x10^4$ cells/cm^2). After 24 hours, the medium was changed to Osteoblast Differentiation Medium (ZenBio, NC, USA) and the differentiation was allowed to proceed for 21days, with the medium changed every 3-4 days. Cells monolayers were fixed in graded ethanol concentrations (25, 50, 75, 100% in PBS) and incubated with alizarin red S (Sigma-Aldrich, Gillingham, UK) at pH 4.2 for 10 minutes to identify calcium deposits. All images were taken using a Leica DMIL microscope (Leica Microsystems, Milton Keynes, UK) with Nikon DS-Fi1 camera (Kingston Upon Thames, UK). These experiments were repeated independently 2-3 times.

Myogenic and neuronal differentiation

GO cells were seeded on glass coverslips ($2x10^3$ cells/cm^2) in standard medium in 6 well plates. After 24 hours, the medium was supplemented with TGF-β1 (100 ng/ml, PeproTech, London, UK) for 48 hours (myogenic differentiation) or with neuronal differentiation inducer III (20 μM, Calbiochem, Merck KGaA, Darmstadt, Germany) for 5 days (neurogenic differentiation). The coverslips were then fixed in 3.7% formaldehyde, permeabilised in 0.5% Triton-X100 (Sigma-Aldrich, Gillingham, UK), washed with 0.1M glycine, and blocked with 1% FBS and 1% donkey serum in Tris Buffer Saline [21]. Cells were incubated with primary antibodies against α-smooth muscle actin (α-SMA, mouse, 1:50; Sigma-Aldrich, Gillingham, UK) and neuron specific β III tubulin (rabbit, 1:200; Abcam, Cambridge, UK), followed by anti-mouse tetramethylrhodamine (TRITC)-conjugated and anti-rabbit fluorescein isothiocyanate

(FITC)-conjugated secondary antibodies (both donkey, 1:100; Jackson Labs, Maine, USA) respectively. Following washes, the coverslips were mounted with Fluoroshield mounting medium with DAPI (Abcam, Cambridge, UK). Cells were imaged using a NIKON Ti-E microscope with CoolSNAP HQ2 camera (Photometrics, AZ, USA), using a 20X air objective (20X Plan Fluor ELWD ADM with correction collar).

Real-time Polymerase Chain Reaction (RT-PCR)

Differentiated HO1, HO2 and HO3 cells (osteogenesis and chondrogenesis as above), matching undifferentiated control cells grown under the same conditions but in the standard medium, and cells from standard monolayer cultures were homogenised in 700 µl of Trizol (Thermo Fischer Scientific, Paisley, UK). RNA was extracted using the miRNeasy kit (QIAGEN, Hilden, Germany) according to the manufacturer's instructions. RNA concentration and purity was analysed using NanoDrop 2000 (Thermo Scientific, DE, USA). 200 ng of RNA was then reverse-transcribed using QuantiTect Reverse Transcription kit (QIAGEN, Hilden, Germany) according to the manufacturer's instructions, except for the incubation time at 42°C, which was increased from 15 to 30 minutes. 60 µl of water was then added to the reaction, and 5 µl of this was mixed with 6.25 µl of water, 12.5 µl of TaqMan gene expression master mix (Applied Biosystems, DE, USA) and 1.25 µl of a primer targeting one of the following sequences: aggrecan (ACAN, Hs00153936_m1), SOX-9 (SOX9, Hs01001343_g1), osteonectin (SPARC, Hs00234160_m1), osteocalcin (BGLAP, Hs01587814_g1), Hypoxanthine-guanine phosphoribosyltransferase (HPRT1, Hs02800695_m1), Splicing factor 3A subunit 1 (SF3A1, Hs01066327_m1; all from Applied Biosystems, DE, USA). The real-time PCR settings were as follows: 50°C for 2 minutes, 95°C for 10 minutes, 40 iterations of 95°C for 15 seconds and

60°C for 1 minute. Data interpretation was carried out using the comparative ΔC_T method [22]. Transcription products were then run in 2% agarose gels with 1% TAE buffer in distilled water. Band intensities were measured using ImageJ, and the housekeeping genes HPRT1 (for ACAN and SPARC) or SF3A1 (for SOX9 and BGLAP) were used to normalize the values.

Statistical analysis

Flow cytometry graphs show mean and SEM for three individual experiments. Statistical analysis was performed using ANOVA. Pearson product-moment correlation analysis was performed on averaged flow cytometry results from three separate experiments, and each of the 6 cell lines was shown as a separate data point. Levels of significance were determined using Table of Critical Values for Pearson's correlation coefficient. Statistical analysis for RT-PCR measurements was performed using ANOVA and two-tailed paired student's t-test.

Results

GO orbital fibroblasts display an MSC-like marker profile

One of the criteria used to define MSCs is expression of CD73, CD105 and CD90 in at least 95% of cells, and lack of expression of CD14 or CD11b, CD19 or CD79alpha, CD34, CD45 and HLA-DR in at least 98% of cells [10]. We have shown previously that both GO and control orbital fibroblasts are negative for CD45, but positive for CD90 (57-96 % of the cells), with varying levels of expression [6]. We used here the same fibroblast lines to further analyse the expression of CD73, CD105, CD14, CD19, CD34 and HLA-DR. In addition, CD221 (IGF-1R) was used as a positive control/disease marker, as IGF-1R was previously shown to be overexpressed in GO fibroblasts, underlying some aspects of the disease [23-25].

As expected, a significant proportion of GO fibroblasts expressed CD221 on average, as opposed to less than 20% for control fibroblasts (Figure 1A, B), and the levels expressed by positive cells were significantly higher in GO cells (Figure 1C). Control and GO fibroblasts displayed very high expression levels for positive markers CD73 and CD105 in the majority of the cells (Figure 1A, B), but both the percentage of positive cells and the geometric mean fluorescence intensity of the positive cells were significantly higher in GO fibroblasts (Figure 1B,C).

Only a minor fraction of cells expressed CD14 (0-7.4%), CD19 (0-1.6%) and HLA-DR (0-1.2%) and at levels barely above background. CD34 expression was unexpectedly elevated, with 64.6% (SEM=4.6) of CO cells and 51.3% (SEM=3.6) of GO cells displaying the marker (Figure 1A, B), although the levels of expression were significantly lower in GO cells (Figure 1C).

In order to determine the relationship between CD34 and CD221, and positive markers of MSCs, we analysed separate marker expression using Pearson product-moment correlation (Figure 2). There was a strong, negative correlation between levels of expression of CD34 and CD105 ($r = -0.81$, $p<0.05$; Figure 2A). Conversely, there was a strong positive correlation between the percentages of cells expressing CD221 and positive MSC markers CD73 ($r=0.96$, $p<0.01$) and CD105 ($r=0.88$, $p<0.05$; Figure 2B). Similarly, levels of the expression of CD73 and CD105 markers were strongly correlated to CD221 expression levels ($r=0.84$ and $r=0.87$ respectively, $p<0.05$; Figure 2C). Overall, this showed that GO fibroblasts had a marker profile that more closely resembled a typical MSC profile than that of control orbital fibroblasts, suggesting that GO fibroblasts may comprise an MSC-like population capable of multi-lineage differentiation.

GO orbital fibroblasts undergo lineage specific differentiation

We have previously shown that GO fibroblasts (HO1, HO2, HO3 lines as used here) undergo adipogenesis, both following standard stimulation with adipogenic differentiation medium in monolayer cultures, as well as spontaneously (without any chemical stimulation) when grown within 3 dimensional collagen matrices [6]. To further explore the differentiation potential of GO fibroblasts, we tested the cells for chondrogenic, osteogenic, myogenic and neurogenic potential. Following osteogenic differentiation for 21 days, alizarin red was used to stain calcium deposits that characterise bone mineral formations. Clusters of stained deposits were found in all 3 GO cell lines incubated in osteogenesis differentiation medium (Figure 3, A-C) but not in control medium (Figure 3, D-E). Additionally, the differentiated cells looked more

226 irregular, forming clusters of cells with a 3-dimensional aspect as compared to the characteristic
227 flat, spindle-shaped morphology of the cells in control medium (Figure 3, A-F).

228 Following chondrogenic differentiation in cell pellets for 21 days, we used alcian blue
229 staining to evaluate glycosaminoglycan production as a late chondrogenesis marker. Alcian blue
230 produced a strong blue staining in the pellets incubated in differentiation medium (Figure 3, G-I),
231 suggesting significant chondrogenic differentiation, whilst only faint blue spots were visible in
232 the control pellets (Figure 3, J-L). The Alcian blue staining was largely absent when the sections
233 were treated with hyaluronidase prior to staining (Figure 3, G'-L'), suggesting that most of the
234 staining in the samples was due to the presence of glycosamiglycans (rather than non specific
235 binding of the dye to lipids).

236 Osteogenesis and chondrogenesis were confirmed by analysing the expression of specific
237 differentiation markers, BGLAP and SPARC for the former, and ACAN and SOX9 for the latter
238 respectively. Both real-time PCR (Supplementary Table 1) and the subsequent gel
239 electrophoresis (Figure 4 and Supplementary Figure 3) identified differentiation markers in all
240 three fibroblasts cell lines. All cells cultured according to the differentiation protocols showed
241 upregulation of BGLAP ($p=0.006$) and SOX9 ($p=0.05$), with upregulation of ACAN seen in
242 HO1 and HO2, and upregulation of SPARC seen in HO3.

243 TGF-β is a potent inducer of myogenic differentiation of MSCs [26, 27], and we found that
244 stimulation of GO cells with TGF-β led to a marked increase in α-SMA expression (marking the
245 onset of myocyte differentiation), as well as its significant incorporation into actin stress fibres
246 (Figure 5, A-F). After differentiation towards neuronal lineage using neuronal differentiation
247 inducer III, the cells adopted a more elongated morphology (Figure 5, G-L), with some of them
248 displaying long neuron-like protrusions (Figure 5I). However, both differentiated and

249 undifferentiated cells expressed the neuron-specific beta-III tubulin marker, suggesting a pre-
250 existing commitment towards a neuronal lineage (Figure 5, G-L).

Discussion

The presence of stem cells within adipose tissue is well established and this includes orbital adipose tissue, where pluripotent cells have been identified that display a classical multi-lineage potential as well as the more unusual ability to differentiate into corneal epithelial cells [13, 14, 28]. In addition, there is increasing evidence that fibroblasts display characteristics that define MSCs, including immuno-phenotype and multi-lineage differentiation [29-32], and that differences between classical MSC and fibroblasts are within variability seen amongst MSC lines of different topographical origin [30, 33, 34]. We have previously shown that primary fibroblasts from the orbit of patients with active Graves' disease displayed a dual profibrotic/contractile and adipogenic phenotype when cultured within 3 dimensional (3D) collagen matrices [6], and produced hyaluronan when stimulated with IGF1 or patient serum (D. Ezra, unpublished data). These cells were also largely positive for CD90 and negative for CD45 [6], both positive and negative markers of MSCs respectively [10-12]. We thus hypothesized that GO orbital fibroblasts contain a population of cells capable of pluripotent differentiation, potentially underlying the multifaceted phenotype of the disease.

We show here that GO fibroblasts fulfil most of the proposed minimal criteria for MSC identification [10]: they are adherent to plastic under normal culture conditions, and express CD90 [6], CD73, CD105 whilst lacking the expression of CD45 [6], CD14, CD19 and HLA-DR. However, a significant proportion of both control and GO orbital cells expressed CD34, a commonly used negative marker of MSCs, albeit to low levels. Despite being often acknowledged as a negative marker for MSCs [10], both adipose-derived MSCs (AMSCs) and committed pre-adipocytes have been shown to express CD34 [12]. Thus the presence of CD34 positive cells within a putative MSC compartment in GO fibroblasts may be linked to the cells' pro-adipogenic phenotype and

spontaneous adipogenic differentiation potential in 3D cultures [6]. In addition, the presence/absence of CD34 on MSCs may depend on how, and where from, the cells have been isolated [35-37], and indeed, CD34 was previously found expressed in orbital adipose tissue, particularly in the nasal fat area [14]. Alternatively, CD34 positive cells may comprise a subpopulation of fibrocytes, having invaded the orbit from the circulation and contributing to the diversity of the orbital fibroblast phenotype [8], and to the local MSC pool[36]. Although fibrocytes are normally CD45 positive and our GO populations have been found largely negative for CD45[6], we cannot entirely rule out some fibrocyte involvement as the expression of CD45 in fibrocytes is known to decrease after they enter the tissue *in vivo* as well as during culture *in vitro* [38]. Overall however, when marker profiles were analysed for correlations, the frequency of the positive MSC markers CD105 and CD73 correlated positively with the presence of CD221 (IGF-1R), a marker that has been implicated in the pathology of the disease[24]. Conversely, CD34 expression was inversely correlated to the positive markers expression. This suggests that the increased expression of MSC positive markers and correlated decrease in MSC negative markers in GO orbital fibroblasts reflect the emergence within these cells of a population with MSC characteristics that may be linked disease progression.

When probed for their lineage specific differentiation abilities, GO fibroblasts showed MSC-like pluripotency. In addition to their previously shown ability to differentiate into adipocytes [5, 6, 9], we show here that GO fibroblasts displayed significant levels of osteogenesis and chondrogenesis. Both RT-PCR quantitation and gene electrophoresis confirmed the presence of differentiation markers (BGLAP and SPARC for osteogenesis; ACAN and SOX9 for chondrogenesis) in all three GO lines, in both cells exposed to the differentiation protocol and cells grown in control medium. BGLAP and SOX9, which were expressed at lower levels than

297 the other markers, were significantly upregulated in differentiated cells, confirming the
298 differentiation towards osteogenesis and chondrogenesis respectively. A possible explanation for
299 the lack of significant upregulation of the other markers in response to the differentiation
300 protocols is the high basal level of expression. As cell density has been reported to play a role in
301 both osteogenesis [39, 40] and chondrogenesis [41, 42], we additionally tested expression of three of the
302 markers in cells grown under standard conditions, i.e. as subconfluent monolayers. Again, all
303 markers tested were present in the cells, but most of them at levels lower than in the cells that
304 had undergone differentiation (ACAN: $p=0.04$; BGLAP, SPARC, SOX9: $p> 0.05$). Therefore,
305 we propose that GO fibroblasts may constitutively express markers classically considered as
306 markers for osteo- and chondrogenesis, but a further differentiation procedure may be required to
307 induce functional differentiation and production of calcium deposits and hyaluronan. Indeed
308 SPARC expression in both mouse and human fibroblasts has been linked to skin and lung
309 fibrosis [43, 44], suggesting that constitutive expression of SPARC in GO fibroblasts may be linked
310 to their pro-fibrotic phenotype.
311
312 Myogenic differentiation was not originally one of the minimal criteria that define MSCs.
313 Nevertheless, a number of studies have shown that MSCs could differentiate into the myogenic
314 lineage, including both smooth and striated muscle, under various conditions [45-48]. Although both
315 α-SMA and MyoD have been described as early myogenic markers, there is some evidence that
316 MyoD expression could be transient [46]. In addition, α-SMA has been linked to fibrosis, which
317 could again be of significant relevance in the pathology of Graves' orbitopathy. GO cells
318 displayed minimal expression levels of α-SMA in normal cultures but all three lines showed
319 significantly elevated levels of α-SMA, as well as its incorporation into strong actin stress fibres,

denoting a differentiation towards a myofibroblast/myogenic phenotype. This strong response to TGFβ stimulation may also be linked to the pro-fibrotic phenotype of the cells [6], possibly underlying some of the fibrotic pathology in GO. The ability of MSCs to differentiate into neurons is more controversial [49], but we found that GO fibroblasts appear to gain some morphological characteristics of neuronal cells upon stimulation with neuronal differentiation inducer III. However, they spontaneously expressed the neuronal marker β-III tubulin with little, if any, changes following stimulation with neuronal differentiation inducer III. This may be a reflection of the peculiar embryonic origin of orbital fat, as craniofacial adipose tissue is thought to originate from the neural crest cells rather than the mesoderm as for the most of the white adipose tissue [50, 51].

Overall, our findings suggest that GO orbital fibroblasts populations comprise cells that broadly fulfil the criteria defining MSCs, and have the potential for multi-lineage differentiation. Although this study is still preliminary and it is not clear whether the pluripotent cell population in GO represents true MSCs (with self-renewal potential), progenitors, or a mix of both, the identification of such cells suggests that they could underlie some of the complexity of the disease phenotype. Considering the emerging evidence of a role for MSCs in modulating inflammation, and particularly in the context of autoimmune diseases [52], it is tantalizing to speculate that MSCs/progenitors could be an important factor controlling disease progression in GO, as they have been proposed to for other fibrotic diseases [50].

Acknowledgments

The authors wish to thank Grazyna Galatowicz for help with the FACS analysis.

References

1. Trobe JD. Optic nerve involvement in dysthyroidism. Ophthalmology. 1981; **88**(6): 488-92.

2. Tallstedt L, Lundell G, Torring O, Wallin G, Ljunggren JG, Blomgren H, et al. Occurrence of ophthalmopathy after treatment for Graves' hyperthyroidism. The Thyroid Study Group. N Engl J Med. 1992; **326**(26): 1733-8.

3. El-Kaissi S, Frauman AG, Wall JR. Thyroid-associated ophthalmopathy: a practical guide to classification, natural history and management. Intern Med J. 2004; **34**(8): 482-91.

4. Regensburg NI, Wiersinga WM, Berendschot TT, Potgieser P, Mourits MP. Do subtypes of graves' orbitopathy exist? Ophthalmology. 2011; **118**(1): 191-6.

5. Eckstein AK, Johnson KT, Thanos M, Esser J, Ludgate M. Current insights into the pathogenesis of Graves' orbitopathy. Horm Metab Res. 2009; **41**(6): 456-64.

6. Li H, Fitchett C, Kozdon K, Jayaram H, Rose GE, Bailly M, et al. Independent adipogenic and contractile properties of fibroblasts in graves' orbitopathy: an in vitro model for the evaluation of treatments. PLoS One. 2014; **9**(4): e95586.

7. Ezra DG, Rose GE, Bailly M. Developing an in vitro model of tissue expansion in Graves ophthalmopathy: exploring the role of IGF1 receptor targeting as a novel treatment Endocrine Abstracts 2011; **25**(OC1.4).

8. Smith TJ. Potential role for bone marrow-derived fibrocytes in the orbital fibroblast heterogeneity associated with thyroid-associated ophthalmopathy. Clinical and experimental immunology. 2010; **162**(1): 24-31.

9. Koumas L, Smith TJ, Feldon S, Blumberg N, Phipps RP. Thy-1 expression in human fibroblast subsets defines myofibroblastic or lipofibroblastic phenotypes. Am J Pathol. 2003; **163**(4): 1291-300.

10. Dominici M, Le Blanc K, Mueller I, Slaper-Cortenbach I, Marini F, Krause D, et al. Minimal criteria for defining multipotent mesenchymal stromal cells. The International Society for Cellular Therapy position statement. Cytotherapy. 2006; **8**(4): 315-7.

11. Huang SJ, Fu RH, Shyu WC, Liu SP, Jong GP, Chiu YW, et al. Adipose-derived stem cells: isolation, characterization, and differentiation potential. Cell Transplant. 2013; **22**(4): 701-9.

12. Cawthorn WP, Scheller EL, MacDougald OA. Adipose tissue stem cells meet preadipocyte commitment: going back to the future. J Lipid Res. 2012; **53**(2): 227-46.

13. Ho JH, Ma WH, Tseng TC, Chen YF, Chen MH, Lee OK. Isolation and characterization of multi-potent stem cells from human orbital fat tissues. Tissue Eng Part A. 2011; **17**(1-2): 255-66.

14. Korn BS, Kikkawa DO, Hicok KC. Identification and characterization of adult stem cells from human orbital adipose tissue. Ophthal Plast Reconstr Surg. 2009; **25**(1): 27-32.

15. Tabatabaei M, Mosaffa N, Nikoo S, Bozorgmehr M, Ghods R, Kazemnejad S, et al. Isolation and partial characterization of human amniotic epithelial cells: the effect of trypsin. Avicenna J Med Biotechnol. 2014; **6**(1): 10-20.

16. De Francesco F, Tirino V, Desiderio V, Ferraro G, D'Andrea F, Giuliano M, et al. Human CD34/CD90 ASCs are capable of growing as sphere clusters, producing high levels of VEGF and forming capillaries. PLoS One. 2009; **4**(8): e6537.

17. Mulder WM, Koenen H, van de Muysenberg AJ, Bloemena E, Wagstaff J, Scheper RJ. Reduced expression of distinct T-cell CD molecules by collagenase/DNase treatment. Cancer Immunol Immunother. 1994; **38**(4): 253-8.

18. Muczynski KA, Ekle DM, Coder DM, Anderson SK. Normal human kidney HLA-DR-expressing renal microvascular endothelial cells: characterization, isolation, and regulation of MHC class II expression. Journal of the American Society of Nephrology : JASN. 2003; **14**(5): 1336-48.

19. Jena B, Maiti S, Huls H, Singh H, Lee DA, Champlin RE, et al. Chimeric antigen receptor (CAR)-specific monoclonal antibody to detect CD19-specific T cells in clinical trials. PLoS One. 2013; **8**(3): e57838.

20. Solchaga LA, Penick KJ, Welter JF. Chondrogenic differentiation of bone marrow-derived mesenchymal stem cells: tips and tricks. Methods Mol Biol. 2011; **698**: 253-78.

21. Bailly M, Macaluso F, Cammer M, Chan A, Segall JE, Condeelis JS. Relationship between Arp2/3 complex and the barbed ends of actin filaments at the leading edge of carcinoma cells after epidermal growth factor stimulation. J Cell Biol. 1999; **145**(2): 331-45.

22. Schmittgen TD, Livak KJ. Analyzing real-time PCR data by the comparative C(T) method. Nat Protoc. 2008; **3**(6): 1101-8.

23. Smith TJ, Hegedus L, Douglas RS. Role of insulin-like growth factor-1 (IGF-1) pathway in the pathogenesis of Graves' orbitopathy. Best Pract Res Clin Endocrinol Metab. 2012; **26**(3): 291-302.

24. Naik VM, Naik MN, Goldberg RA, Smith TJ, Douglas RS. Immunopathogenesis of thyroid eye disease: emerging paradigms. Survey of ophthalmology. 2010; **55**(3): 215-26.

25. Pritchard J, Han R, Horst N, Cruikshank WW, Smith TJ. Immunoglobulin activation of T cell chemoattractant expression in fibroblasts from patients with Graves' disease is mediated through the insulin-like growth factor I receptor pathway. Journal of immunology. 2003; **170**(12): 6348-54.

26. Jeon ES, Moon HJ, Lee MJ, Song HY, Kim YM, Bae YC, et al. Sphingosylphosphorylcholine induces differentiation of human mesenchymal stem cells into smooth-muscle-like cells through a TGF-beta-dependent mechanism. Journal of cell science. 2006; **119**(Pt 23): 4994-5005.

27. Kinner B, Zaleskas JM, Spector M. Regulation of smooth muscle actin expression and contraction in adult human mesenchymal stem cells. Experimental cell research. 2002; **278**(1): 72-83.

28. Wester S. Orbital Stem Cells. Curr Ophthalmol Rep. 2014; **2**(3): 107-15.

29. Blasi A, Martino C, Balducci L, Saldarelli M, Soleti A, Navone SE, et al. Dermal fibroblasts display similar phenotypic and differentiation capacity to fat-derived mesenchymal stem cells, but differ in anti-inflammatory and angiogenic potential. Vasc Cell. 2011; **3**(1): 5.

30. De Luca A, Verardi R, Neva A, Benzoni P, Crescini E, Xia E, et al. Comparative Analysis of Mesenchymal Stromal Cells Biological Properties. ISRN Stem Cells. 2013; **2013**: 9.

31. Lorenz K, Sicker M, Schmelzer E, Rupf T, Salvetter J, Schulz-Siegmund M, et al. Multilineage differentiation potential of human dermal skin-derived fibroblasts. Exp Dermatol. 2008; **17**(11): 925-32.

32. Sabatini F, Petecchia L, Tavian M, Jodon de Villeroche V, Rossi GA, Brouty-Boye D. Human bronchial fibroblasts exhibit a mesenchymal stem cell phenotype and multilineage

differentiating potentialities. Laboratory investigation; a journal of technical methods and pathology. 2005; **85**(8): 962-71.

33. Hematti P. Mesenchymal stromal cells and fibroblasts: a case of mistaken identity? Cytotherapy. 2012; **14**(5): 516-21.

34. Wagner W, Wein F, Seckinger A, Frankhauser M, Wirkner U, Krause U, et al. Comparative characteristics of mesenchymal stem cells from human bone marrow, adipose tissue, and umbilical cord blood. Experimental Hematology. 2005; **33**(11): 1402-16.

35. Lin CS, Ning H, Lin G, Lue TF. Is CD34 truly a negative marker for mesenchymal stromal cells? Cytotherapy. 2012; **14**(10): 1159-63.

36. Diaz-Flores L, Gutierrez R, Garcia MP, Saez FJ, Diaz-Flores L, Jr., Valladares F, et al. CD34+ stromal cells/fibroblasts/fibrocytes/telocytes as a tissue reserve and a principal source of mesenchymal cells. Location, morphology, function and role in pathology. Histol Histopathol. 2014.

37. Sidney LE, Branch MJ, Dunphy SE, Dua HS, Hopkinson A. Concise review: evidence for CD34 as a common marker for diverse progenitors. Stem Cells. 2014; **32**(6): 1380-9.

38. Keeley EC, Mehrad B, Strieter RM. The role of fibrocytes in fibrotic diseases of the lungs and heart. Fibrogenesis Tissue Repair. 2011; **4**: 2.

39. Song W, Lu HX, Kawazoe N, Chen GP. Gradient patterning and differentiation of mesenchymal stem cells on micropatterned polymer surface. J Bioact Compat Pol. 2011; **26**(3): 242-56.

40. Kim K, Dean D, Mikos AG, Fisher JP. Effect of Initial Cell Seeding Density on Early Osteogenic Signal Expression of Rat Bone Marrow Stromal Cells Cultured on Cross-Linked Poly(propylene fumarate) Disks. Biomacromolecules. 2009; **10**(7): 1810-7.

41. Haas AR, Tuan RS. Chondrogenic differentiation of murine C3H10T1/2 multipotential mesenchymal cells: II. Stimulation by bone morphogenetic protein-2 requires modulation of N-cadherin expression and function. Differentiation. 1999; **64**(2): 77-89.

42. Tsonis PA, Goetinck PF. Cell-Density Dependent Effect of a Tumor Promoter on Proliferation and Chondrogenesis of Limb Bud Mesenchymal Cells. Experimental Cell Research. 1990; **190**(2): 247-53.

43. Zhou X, Tan FK, Guo X, Arnett FC. Attenuation of collagen production with small interfering RNA of SPARC in cultured fibroblasts from the skin of patients with scleroderma. Arthritis and rheumatism. 2006; **54**(8): 2626-31.

44. Wang JC, Lai S, Guo X, Zhang X, de Crombrugghe B, Sonnylal S, et al. Attenuation of fibrosis in vitro and in vivo with SPARC siRNA. Arthritis Res Ther. 2010; **12**(2): R60.

45. Beier JP, Bitto FF, Lange C, Klumpp D, Arkudas A, Bleiziffer O, et al. Myogenic differentiation of mesenchymal stem cells co-cultured with primary myoblasts. Cell Biol Int. 2011; **35**(4): 397-406.

46. Gang EJ, Jeong JA, Hong SH, Hwang SH, Kim SW, Yang IH, et al. Skeletal myogenic differentiation of mesenchymal stem cells isolated from human umbilical cord blood. Stem Cells. 2004; **22**(4): 617-24.

47. Drost AC, Weng S, Feil G, Schafer J, Baumann S, Kanz L, et al. In vitro myogenic differentiation of human bone marrow-derived mesenchymal stem cells as a potential treatment for urethral sphincter muscle repair. Ann N Y Acad Sci. 2009; **1176**: 135-43.

48. Jeon ES, Park WS, Lee MJ, Kim YM, Han J, Kim JH. A Rho kinase/myocardin-related transcription factor-A-dependent mechanism underlies the sphingosylphosphorylcholine-induced

475 differentiation of mesenchymal stem cells into contractile smooth muscle cells. Circulation
476 research. 2008; **103**(6): 635-42.
477 49. Franco Lambert AP, Fraga Zandonai A, Bonatto D, Cantarelli Machado D, Pegas
478 Henriques JA. Differentiation of human adipose-derived adult stem cells into neuronal tissue:
479 does it work? Differentiation. 2009; **77**(3): 221-8.
480 50. Berry DC, Stenesen D, Zeve D, Graff JM. The developmental origins of adipose tissue.
481 Development. 2013; **140**(19): 3939-49.
482 51. Billon N, Iannarelli P, Monteiro MC, Glavieux-Pardanaud C, Richardson WD, Kessaris
483 N, et al. The generation of adipocytes by the neural crest. Development. 2007; **134**(12): 2283-92.
484 52. Singer NG, Caplan AI. Mesenchymal stem cells: mechanisms of inflammation. Annu
485 Rev Pathol. 2011; **6**: 457-78.
486
487

Figure legends

Figure 1. GO and control orbital fibroblasts express MSC markers. The expression of MSC markers CD105, CD73, CD14, CD19, HLA-DR and CD34 [10], as well as CD221 (IGF-1R) was analysed in GO and control fibroblasts using Flow Cytometry. (A) Representative flow charts for individual markers in one GO (line HO1) and one control (line CO2) fibroblast line. Grey areas represent specific marker expression profile, with the percentage of positive cells as indicated. White areas show the distribution of the fluorescence using non-specific matching IgG isoform control. (B, C) Percentage of cells expressing the indicated marker (B) and Geometric Mean Fluorescence Intensity (gMFI) for each marker (C). Shown is the mean +/- SEM for 3 GO and 3 control fibroblast lines, with n=3 for each marker in each cell line. *, statistically significant difference between control and GO cells ($p<0.05$).

Figure 2. MSC marker expression is correlated with disease profile. Pearson product-moment correlation analysis was performed between (A) expression levels (mean gMFI) of CD34 versus CD73 (circles) and CD105 (triangles); (B), percentage of cells expressing CD221 versus CD73 and CD105; and (C) expression levels of CD221 versus CD73 and CD105. Each point represents averaged data (n=3) for each control (filled symbols) and GO (empty symbols) cell line. Statistically significant correlations: * $p<0.05$, ** $p<0.01$.

Figure 3. GO fibroblasts demonstrate osteogenic and chondrogenic lineage differentiation. GO fibroblasts (lines HO1-3) were induced towards osteogenic (A-C), and chondrogenic (G/G'-I/ I') differentiation using specific media or kept in control medium under the same conditions

("undifferentiated"; D-F and J/J'-L/L', respectively). (A-F) Cells were stained with alizarin red in order to evaluate calcium deposits (brown areas). (G-L') Cell pellets were stained with Alcian blue without (G-L) or with (G'-L') prior treatment with hyaluronidase in order to evaluate glycosaminoglycan production (blue areas). Scale bar, 10 μm.

Figure 4. GO fibroblasts express markers of osteogenesis and chondrogenesis. GO fibroblasts (lines HO1-3) were induced towards osteogenic (A, B), and chondrogenic (C, D) differentiation ("differentiated", black bars) or kept in control medium under the same conditions ("undifferentiated", grey bars); additionally, cells grown under standard cell culture conditions were tested (A-C, "standard", white bars). Expression levels of markers of osteogenesis (BGLAP and SPARC) and chondrogenesis (ACAN, SOX9) were assessed by semi-quantitative analysis of agarose gel electrophoresis of RT-PCR products. Shown is the mean +/- SEM, with n=2 for each marker in each cell line.

Figure 5. GO fibroblasts demonstrate myogenic and neuronal lineage differentiation. GO fibroblasts (lines HO1-3) were induced towards myogenic (A-C) and neuronal (G-I) differentiation using specific media or kept in control medium under the same conditions ("undifferentiated"; D-F and J-K respectively). (A-F) Cells were immunostained for α-SMA (red) and DAPI (blue). (G-L) Cells were immunostained for β-III Tubulin (green) and DAPI (blue). Scale bar, 100 μm.

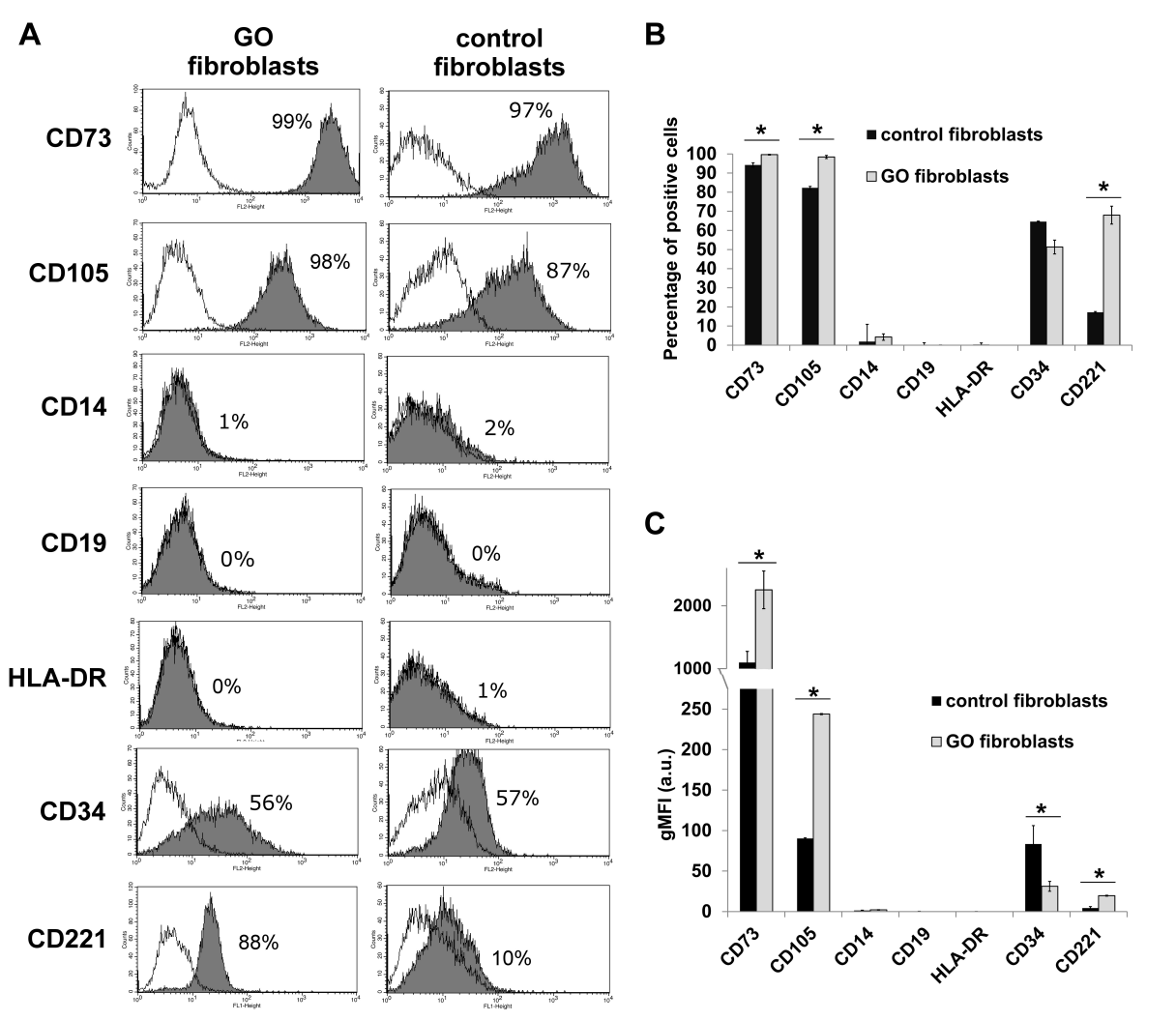
A
GO fibroblasts
control fibroblasts
CD73
99%
97%
CD105
98%
87%
CD14
1%
2%
CD19
0%
0%
HLA-DR
0%
1%
CD34
56%
57%
CD221
88%
10%
B
Percentage of positive cells
control fibroblasts
GO fibroblasts
CD73
CD105
CD14
CD19
HLA-DR
CD34
CD221
C
gMFI (a.u.)
control fibroblasts
GO fibroblasts
CD73
CD105
CD14
CD19
HLA-DR
CD34
CD221

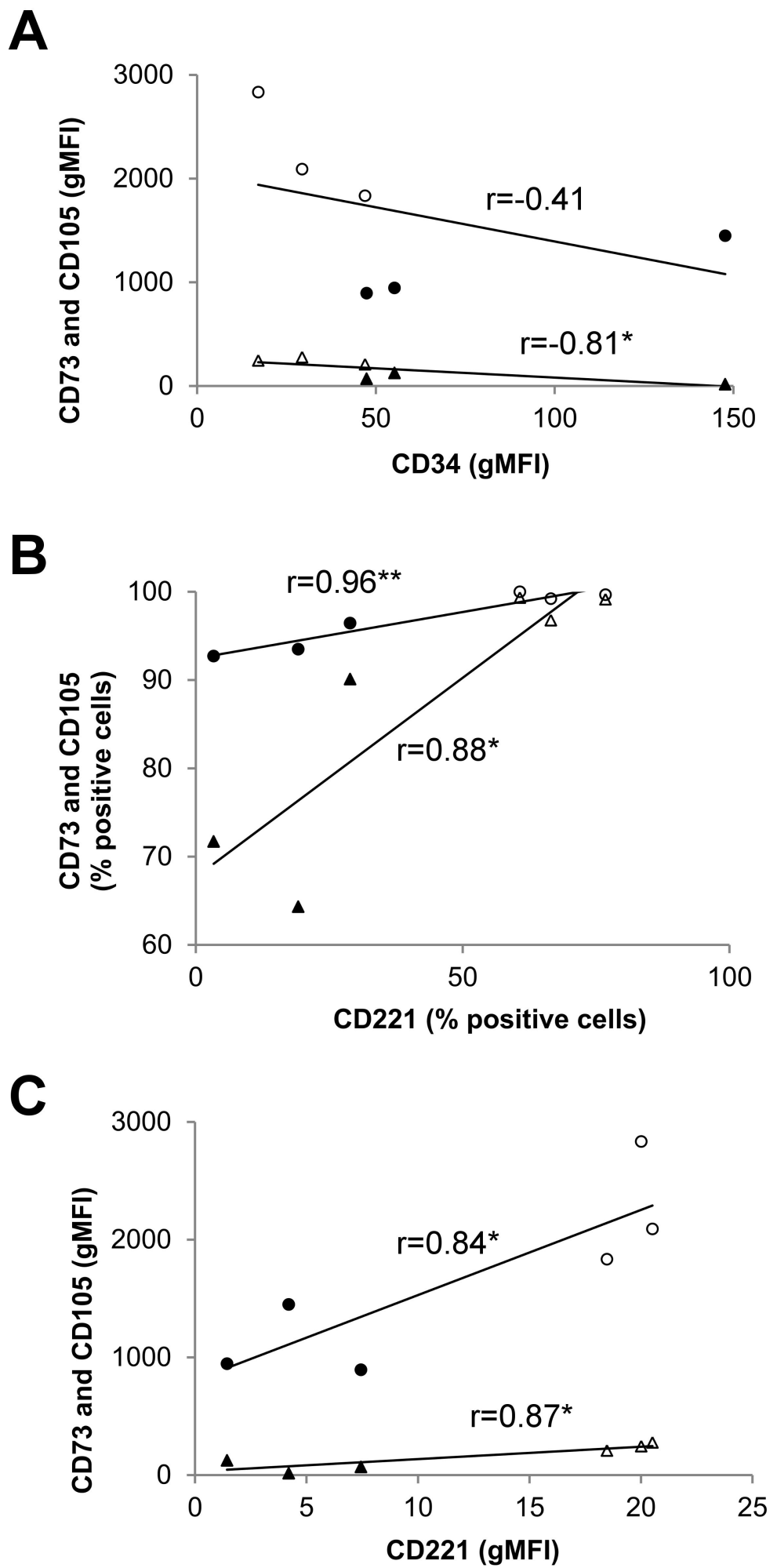
A
3000
2000
1000
0
CD73 and CD105 (gMFI)
r=-0.41
r=-0.81*
0
50
100
150
CD34 (gMFI)
B
100
90
80
70
60
CD73 and CD105 (% positive cells)
r=0.96**
r=0.88*
0
50
100
CD221 (% positive cells)
C
3000
2000
1000
0
CD73 and CD105 (gMFI)
r=0.84*
r=0.87*
0
5
10
15
20
25
CD221 (gMFI)

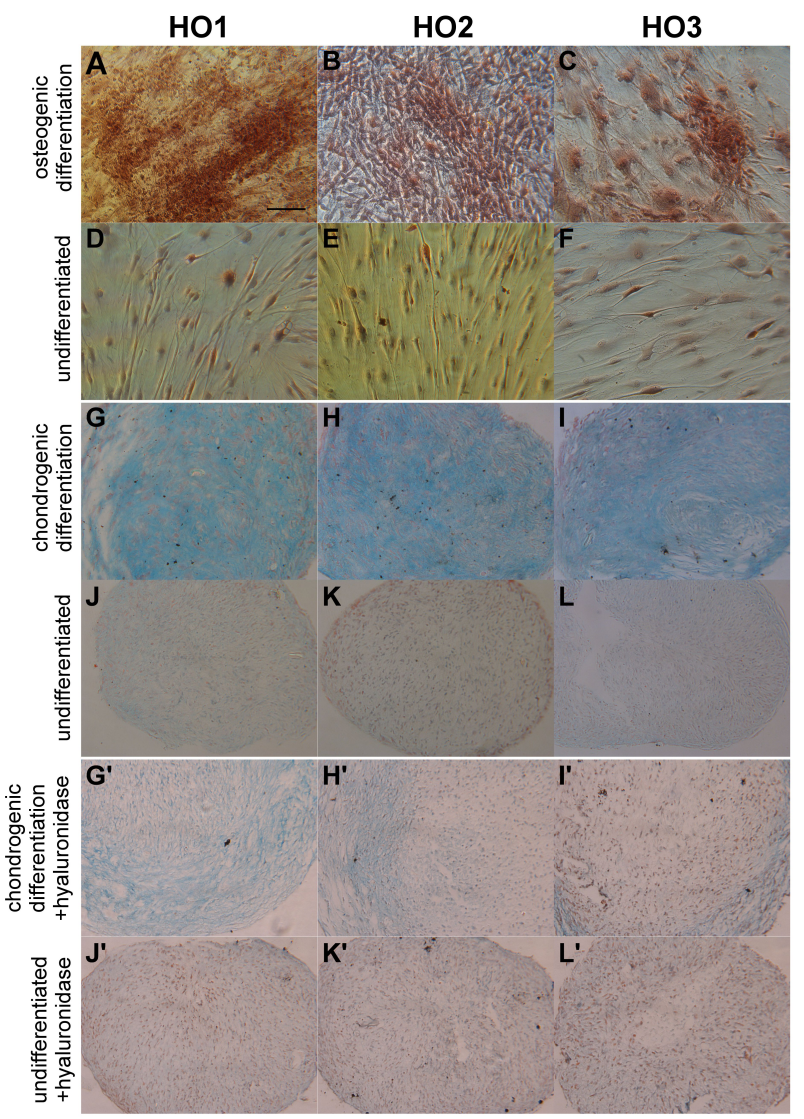
HO1
HO2
HO3
osteogenic differentiation
undifferentiated
chondrogenic differentiation
undifferentiated
chondrogenic differentiation +hyaluronidase
undifferentiated +hyaluronidase
A
B
C
D
E
F
G
H
I
J
K
L
G'
H'
I'
J'
K'
L'

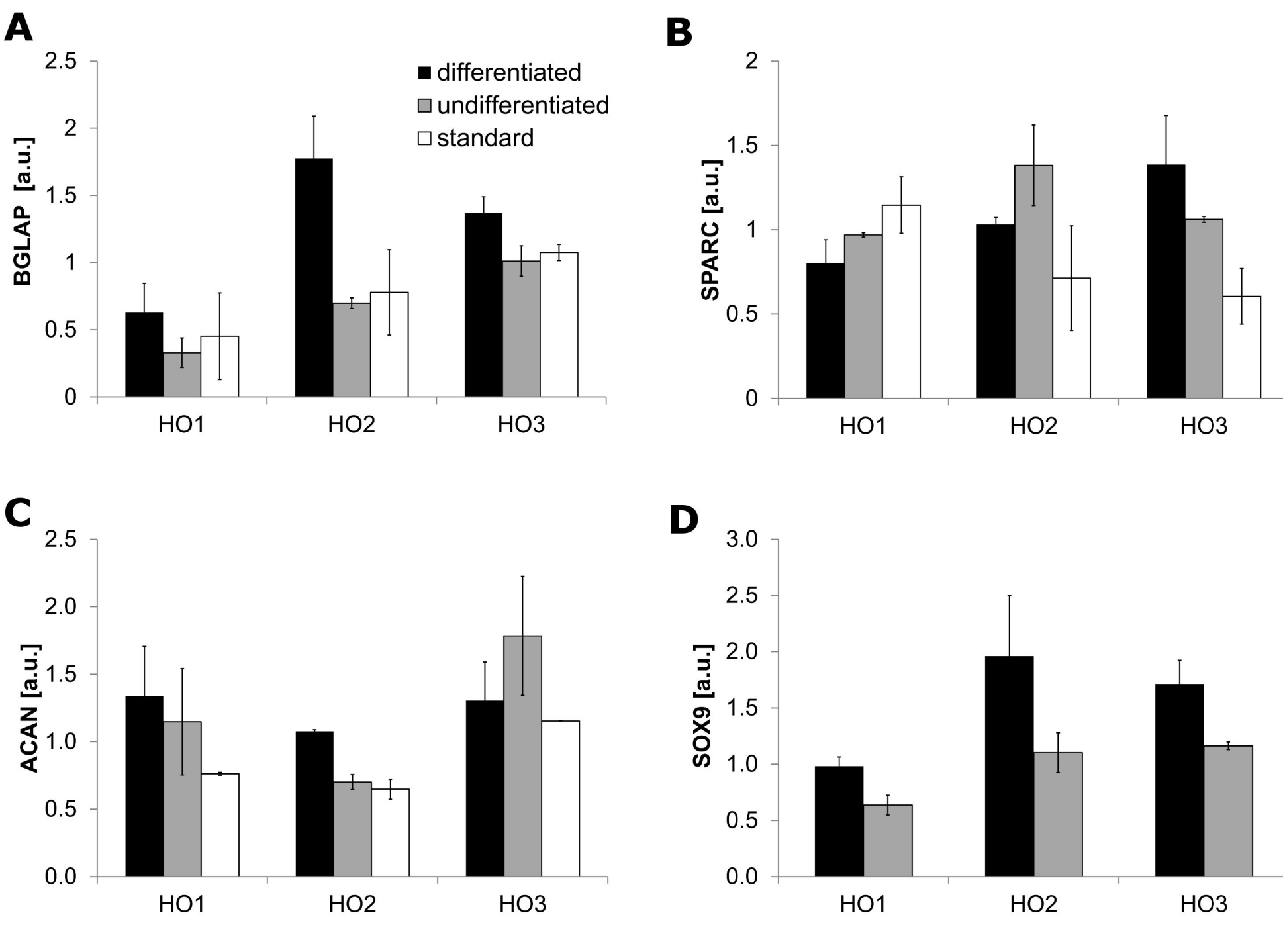
A
B
C
D
differentiated
undifferentiated
standard
BGLAP [a.u.]
SPARC [a.u.]
ACAN [a.u.]
SOX9 [a.u.]
HO1
HO2
HO3
0
0.5
1
1.5
2
2.5
0.0
1.0
2.0
3.0

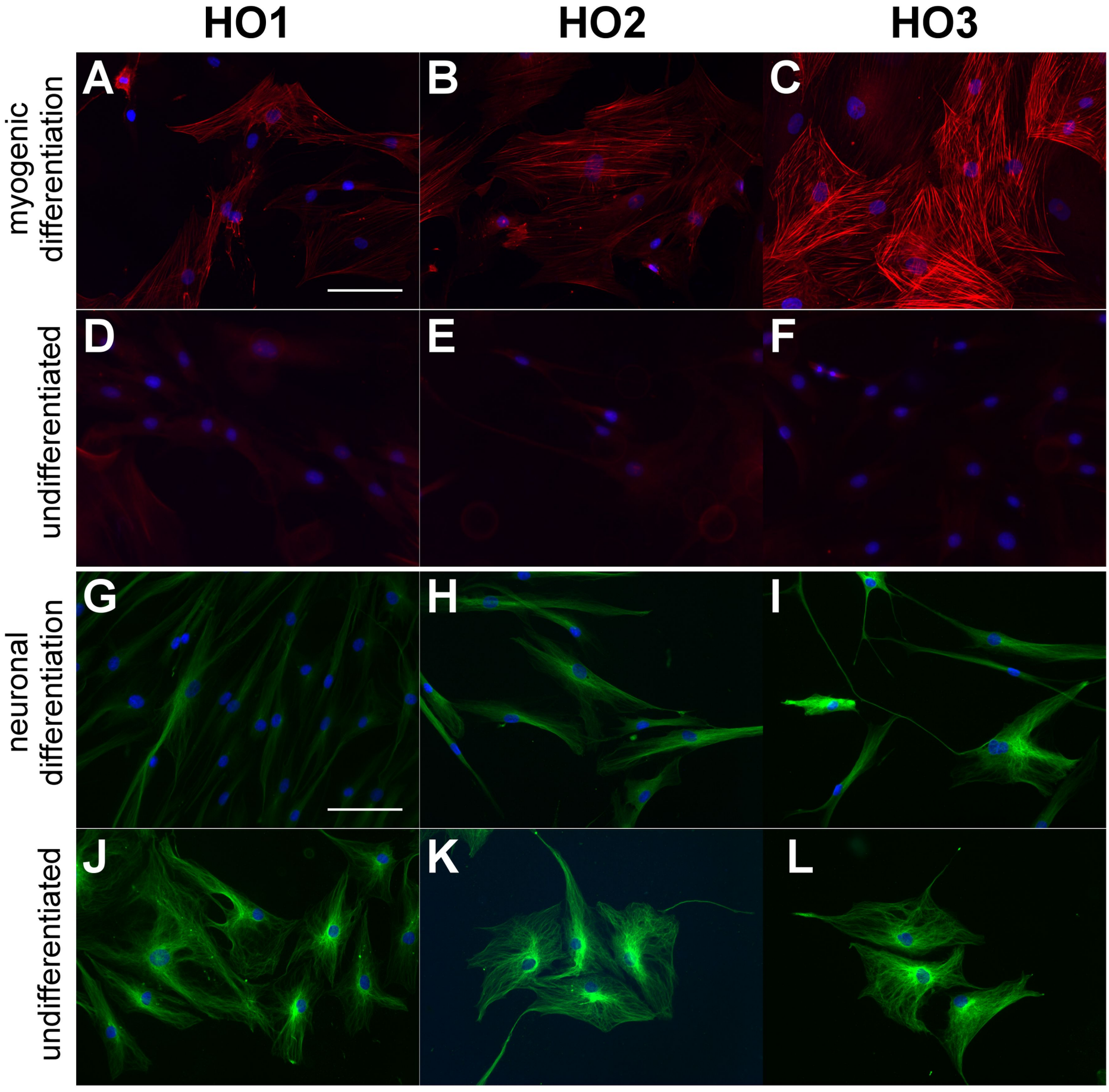
HO1
HO2
HO3
myogenic differentiation
undifferentiated
neuronal differentiation
undifferentiated
A
B
C
D
E
F
G
H
I
J
K
L